

via N-substitution can proceed cleanly, they require relatively long reaction times (1–4 hours) at high reaction concentrations (typically > 1 mM). Herein, we report a new method for chiroptical sensing of various α -amino acids *via* a click-like three-component labeling of primary amines with *o*-phthalaldehyde

and *p*-toluenethiol reagents.⁹ The resulting N-fused aromatic isoindole moiety provides strong UV and CD responses, enabling fast, sensitive, and accurate measurement across a very broad range of analyte concentrations.

Results and discussion

The key to designing dual sensors for CD/UV-based assay is to generate strong and clear readouts for both CD and UV. While a variety of sensing mechanisms have been successfully exploited to amplify the CD signal of α AAAs, methods for simultaneous UV amplification with high sensitivity are surprisingly limited. The three-component condensation reaction between the amino group of α AAAs, *o*-phthalaldehyde (*o*PA) 2, and alkyl thiol reagents such as 2-mercaptopropanoic acid 3a or 3-mercaptopropanoic acid 3b has long been used to derivatize α AAAs for HPLC analysis (Fig. 1A).^{10–12} The *o*PA labeling reactions can proceed cleanly and quickly under mild conditions to form 1-thiolate substituted isoindole product 5. The isoindole moiety has a strong UV absorption around 335 nm, offering a clean UV readout with little background inference from the α AA and the labeling reagents. Its emission around 450 nm has also been used for fluorescence detection. Encouraged by their favorable UV properties, we questioned whether the N-fused isoindole structure on the α AA can induce useful CD signals for chiroptical sensing. The three-component condensation reaction is believed to proceed through a cyclic hemiaminal intermediate 4, which upon dehydration gives the heteroaromatic product.

We commenced the investigation with the reaction of a model α AA L-alanine 1 and a stoichiometric mixture of *o*PA and different thiols. To our delight, the isoindolyl derivatives of Ala indeed exhibited an excellent CD response around 335 nm with *p*-toluenethiol 3e giving the strongest signal among the thiol reagents tested. 3e is a commercially available solid compound and has a much weaker odor than the liquid alkyl thiols. The UV spectrum of the reaction mixture showed a distinct absorption at 335 nm (Fig. 1B).¹³ As indicated by LC-MS and UV measurements, 1.2 equiv. of 3e and 2 reacted cleanly with 1 equiv. of 1 at 2 mM in the mixed solvents of MeOH and phosphate buffer (pH 9) (1/2) at room temperature (rt) under an air atmosphere to give product 5e in $>95\%$ conversion in 1 min. Notably, the use of excess amounts of 2 and 3e (e.g. 3 equiv.) has a negligible impact on the readout of CD and UV at 335 nm (Fig. 1B). The reaction mixture was diluted for CD and UV measurements. UV and LC-MS analyses showed that product 5e is stable over a period of 12 hours.¹⁴ The UV and CD spectra of 5e are not strongly affected by the solvents (see the ESI† for assaying spectra using other organic solvents). Aqueous MeOH medium is preferred for its excellent solubilizing ability for α AAAs and lack of interference for UV and CD measurements.

As shown in Fig. 1C, our preliminary structural and spectroscopic analysis using time-dependent density functional theory (TDDFT) calculations showed that the tolyl group of (*S*)-5e could be positioned below (type (i) conformers) or above (type (ii) conformers) the isoindole plane, forming the opposite

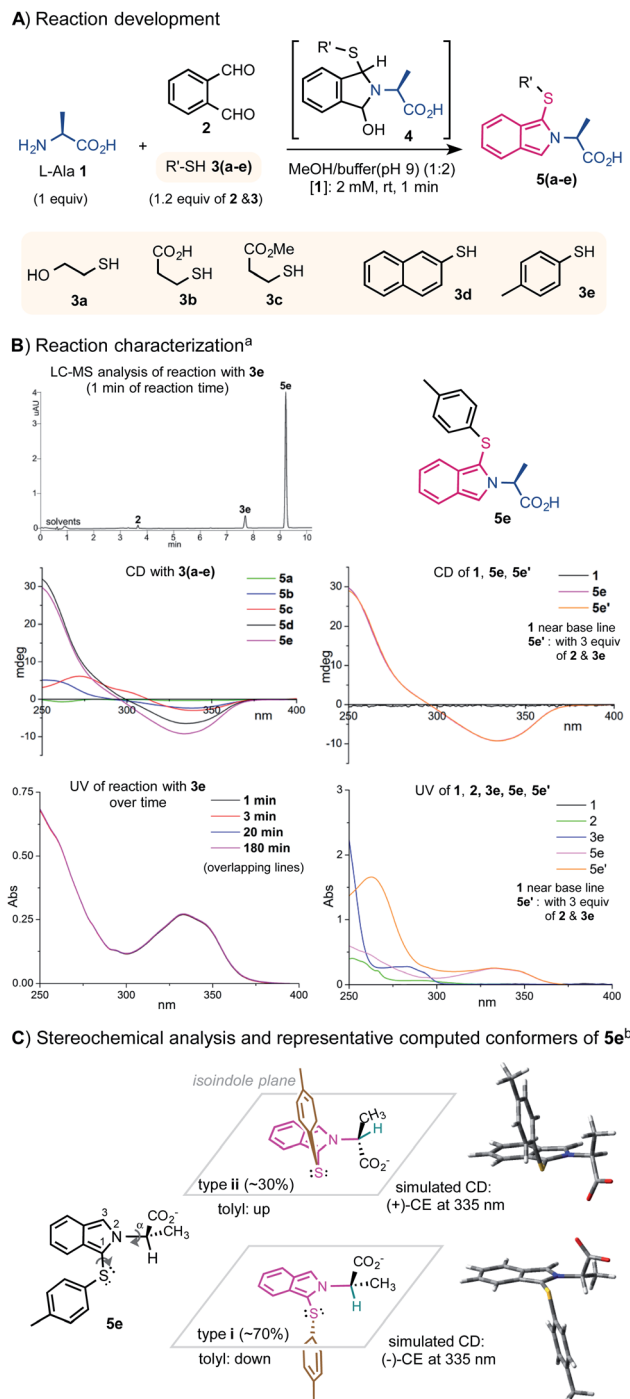


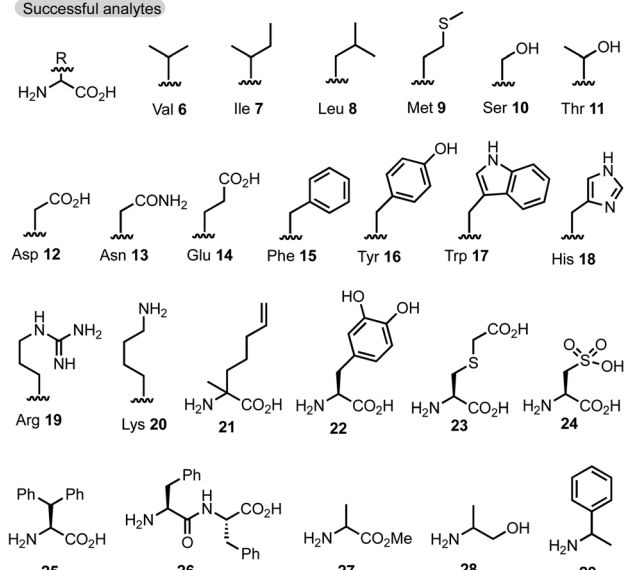
Fig. 1 Labeling of L-Ala with *o*PA and thiols for chiroptical sensing by CD/UV. (A) Reaction development. (B) Reaction characterization; a) reaction mixture was diluted 7 times and samples were measured at 0.285 mM for CD and UV. (C) Stereochemical analysis and representative computed conformers of 5e; b) DFT calculations were performed at the M062X/6-311+G(d,p) level, see the ESI† for details.



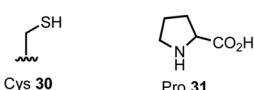
relative stereochemical arrangement of the two aryl groups along the C₁-S bond. Both types (i) and (ii) prefer near-eclipse conformations to the C_α-H bond and adopt *syn* and *anti* to the C₁-S bond respectively. Type (i) and (ii) conformers give opposite Cotton effects (CE) according to the electronic circular dichroism (ECD) simulation. Type (i) conformers are more stable than type (ii) conformers; (i) and (ii) roughly represent 70% and 30% in the conformational equilibrium mixture respectively. The overall ECD spectrum of (*S*)-5e matched well with its experimental data, which showed a negative CE at 335 nm (see ESI Fig. 10† for details).

A) α AA and other chiral amines

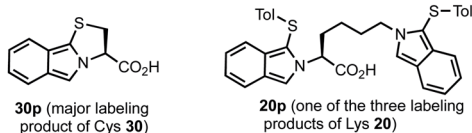
Successful analytes



Problematic analytes



Unusual products^a



B) Selected CD and UV spectra^b

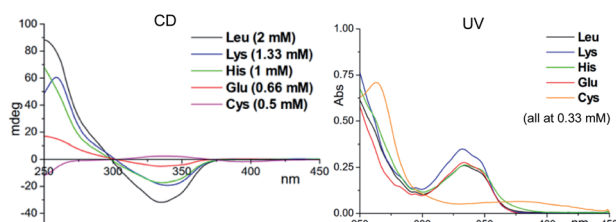


Fig. 2 Substrate scope at a normal concentration range. Standard assaying conditions (1.2 equiv. of reagents, 1 min). (A) α AA and other chiral amines; a) see the ESI† for LC-MS analysis of the reaction mixture. (B) Selected CD and UV spectra; b) samples were measured at the concentration specified.

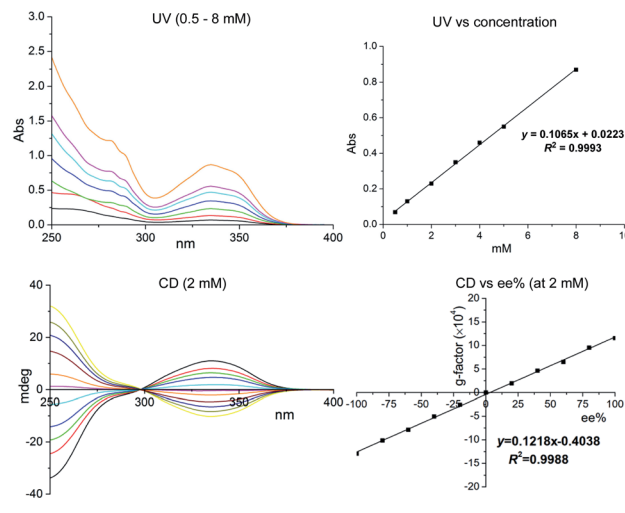
The new protocol was next applied to sense other optically pure proteinogenic α AA and primary alkylamine samples (Fig. 2A). Typically, 1 equiv. of the analytes and 1.2 equiv. of 2 and 3e were mixed in MeOH/buffer at 0.5–8 mM concentration for 1 min. In practice, the assaying can be performed without any deliberate aging. All α As except Cys and Pro showed a similar profile and sensitivity in both CD and UV spectra. The CD and UV spectra of selected α As are shown in Fig. 2B. Pro 31 cannot form the corresponding isoindole product due to its secondary amino group. The reaction of Cys 30 mainly formed a tricyclic isoindole product 30p *via* the intramolecular addition of the SH side chain along with two dimeric side products (see the ESI†). The reaction of Lys 20 with 1.2 equiv. of 2 and 3e gave a mixture of mono- and bis-labeled products (e.g. 20p) at the α and ϵ amino positions (see ESI Fig. 9† for details). Side chains such as CO₂H (Glu, Asp), CONH₂ (Gln, Asn), OH (Ser, Thr, Tyr), guanidine (Arg), and imidazole (His) did not interfere with the condensation reaction. Reactions of nonproteinogenic or unnatural α As 21–25 and even dipeptide Phe-Phe 26 gave similar results. Ala methyl ester 27 gave an almost identical CD readout to Ala 1. Assaying of alaninol 28 and 1-phenylethylamine 29 gave a slightly weaker CD signal (~40%) in comparison with Ala 1.

As shown in Fig. 3A, the UV absorption at 335 nm shows an excellent linear relationship with the concentration of Trp between 0.5 and 8 mM (all samples above 0.5 mM were diluted for CD and UV measurements). Moreover, the CD signals at 335 nm also showed an excellent linear relationship with the enantiomeric excess (ee) of Trp samples assayed at 2 mM using the standard protocol with 1.2 equiv. of oPA and 3e. As shown in Fig. 3B, plots of the *g* factor of CD vs. ee% for representative α As Leu 8, Glu 14, His 18, and Thr 11 measured at 0.33–1 mM showed an excellent linear relationship. The plot of UV absorption vs. concentration showed a notable deviation ($R^2 = 0.9852$) from the linear relationship for Lys probably due to the formation of mixed labeling products (see the ESI†). However, the plot of *g* factor vs. ee% showed excellent linear relationship for Lys.

Chiroptical sensing of analytes at low concentrations remains a difficult challenge for the existing methods due to low labeling reactivity and high background noise. We were pleased to find that our method worked well for α AA samples below 300 μ M under slightly modified conditions with excess amounts of oPA and 3e (5–100 equiv.) and 3 min of mixing time. As exemplified by the test of Ala, the UV signal at 335 nm showed excellent linear relationship with the concentration between 5 and 400 μ M (assaying samples below 0.5 mM were measured without dilution). Moreover, the plot of *g* factor vs. ee% showed an excellent linear relationship for Ala at 10 μ M.¹⁵ Notably, excess amounts of reagents had a negligible impact on the CD and UV signals at 335 nM, due to the unique signal amplifying mechanism of this method. Sensing of the Trp sample at 10 μ M gave similar sensitivity (see the ESI†).

As shown in Table 1, our assay was tested with representative Ala and Trp samples at varied concentrations and of varied enantiomeric ratios. The simple linear relationships greatly simplified the calculation of the concentrations and ee values



A) Test of Trp at normal concentration^a

B) Plots of CD vs ee% of selected αAA

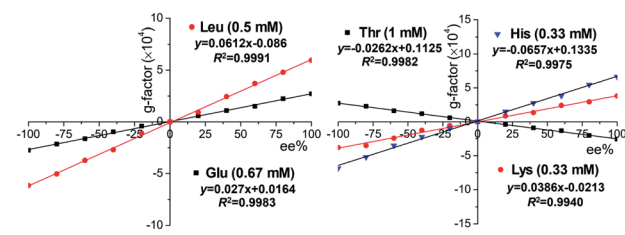
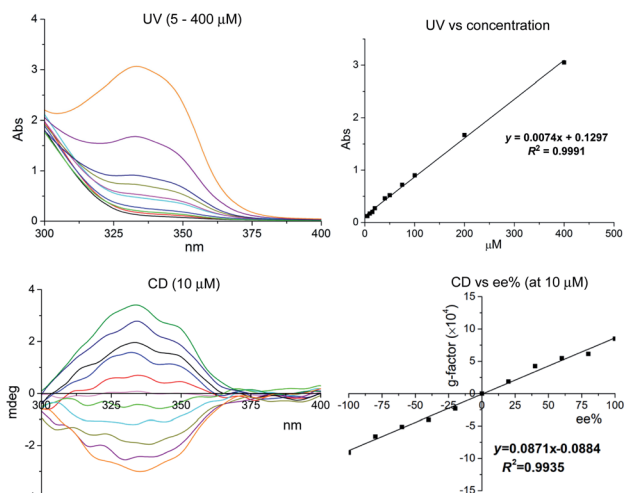
C) Test of Ala at low concentration^b

Fig. 3 Assaying α AAs at varied concentrations. Standard conditions: 1.2 equiv. of 2 and 3e, 1 min for $[\alpha\text{AA}] > 300 \mu\text{M}$. Modified conditions: 5 equiv. and 1 min for 100–300 μM ; 20 equiv. and 3 min for 50–100 μM ; 100 equiv. and 3 min for 5–50 μM . See the ESI† for tests of Trp at 10 μM and Ala at 2 mM. (A) Test of Trp at normal concentration; a) all samples were diluted 6 times for the UV vs. concentration plot. The real measured concentration is 1/6 of the ones shown in the X axis. All samples (2 mM) were diluted 4 times for the CD vs. ee% plot, measured at 0.50 mM. (B) Plots of CD vs. ee% of selected α AA. (C) Test of Ala at low concentration; b) assaying samples were measured without dilution. The g-factor was the average of four measurements.

from UV and CD measurements. In all cases, the absolute configuration of the major enantiomer was correctly assigned. The measured data of concentration and ee values were mostly

Table 1 Chiroptical sensing of Ala and Trp samples at varied concentrations and ee values

Entry	Sample	Sensing				
		Conf.	Conc.	ee%		
1	Ala-L	2.00 mM	-100.0	L	1.91 mM	-98.7
2	Ala-D	7.00 mM	37.1	D	6.87 mM	38.2
3	Trp-L	7.00 mM	-100.0	L	7.10 mM	-103.4
4	Trp-D	3.50 mM	42.8	D	3.57 mM	43.9
5	Ala-L	40.0 μM	-60.0	L	39.2 μM	-61.2
6	Ala-D	10.0 μM	100.0	D	9.5 μM	99.6
7	Trp-L	21.0 μM	-65.0	L	22.2 μM	-67.2
8	Trp-D	38.0 μM	79.0	D	35.8 μM	77.5

within 5% error of the actual value at both high (8 mM) and low (10 μM) assaying concentrations.

Conclusions

In summary, we have developed a highly practical method for comprehensive chiroptical sensing of free α amino acids which gives high sensitivity *via* dual CD/UV measurements using a single instrument. The click-like covalent labeling reaction rapidly fuses the NH_2 group of analytes into a *N*-heteroaromatic isoindole structure, which amplifies both UV and CD signals of amines with an excellent linear relationship with the concentration. The high reactivity and the novel optical reporting mechanism of the labeling reaction allow fast and accurate measurement with negligible aging time and background interference. The sensing assay works well for a remarkably broad range of analyte concentrations with an unprecedented lower limit of 10 micromolar concentration. The sensing assay is simple, robust and cheap. We expect that this method can be readily adapted for high throughput experimentation analysis using a CD instrument equipped with a multiwell plate reader.

Conflicts of interest

There are no conflicts to declare.

Acknowledgements

We gratefully thank the CAMS Innovation Fund for Medical Sciences (CIFMS, No. 2016-I2M-3-009) and the Drug Innovation Major Project (2018ZX09711-001-005) for financial support of this work.

Notes and references

- Selected review of AA sensing: (a) Y. Zhou and J. Yoon, *Chem. Soc. Rev.*, 2012, **41**, 52–67; (b) A. P. F. Turner, *Chem. Soc. Rev.*, 2013, **42**, 3184–3196; (c) M. Tsukamoto and H. B. Kagan, *Adv. Synth. Catal.*, 2002, **344**, 453–463; (d) L. Pu, *Angew. Chem., Int. Ed.*, 2020, **59**, 21814–21828.
- Selected reviews on optical sensing: (a) D. Leung, S. O. Kang and E. V. Anslyn, *Chem. Soc. Rev.*, 2012, **41**,



448–479; (b) J. Wu, B. Kwon, W. Liu, E. V. Anslyn, P. Wang and J. S. Kim, *Chem. Rev.*, 2015, **115**, 7893–7943; (c) B. T. Herrera, S. L. Pilicer, E. V. Anslyn, L. A. Joyce and C. Wolf, *J. Am. Chem. Soc.*, 2018, **140**, 10385–10401; (d) Z. Li, J. R. Askim and K. S. Suslick, *Chem. Rev.*, 2019, **119**, 231–292.

3 Selected examples of fluorescence sensing of AAs: (a) X. Mei and C. Wolf, *J. Am. Chem. Soc.*, 2006, **128**, 13326–13327; (b) Z. Huang, S. Yu, K. Wen, X. Yu and L. Pu, *Chem. Sci.*, 2014, **5**, 3457–3462; (c) E. G. Shcherbakova, T. Minami, V. Brega, T. D. James and P. Anzenbacher Jr, *Angew. Chem., Int. Ed.*, 2015, **54**, 7130–7133; (d) K. Wen, S. Yu, Z. Huang, L. Chen, M. Xiao, X. Yu and L. Pu, *J. Am. Chem. Soc.*, 2015, **137**, 4517–4524; (e) E. G. Shcherbakova, V. Brega, T. Minami, S. Sheykhi, T. D. James and P. Anzenbacher Jr, *Chem.-Eur. J.*, 2016, **22**, 10074–10080.

4 C. Wolf and K. W. Bentley, *Chem. Soc. Rev.*, 2013, **42**, 5408–5424.

5 Selected examples of fluorescence/CD sensing assays: (a) K. W. Bentley and C. Wolf, *J. Am. Chem. Soc.*, 2013, **135**, 12200–12203; (b) K. W. Bentley, Y. G. Nam, J. M. Murphy and C. Wolf, *J. Am. Chem. Soc.*, 2013, **135**, 18052–18055; (c) K. W. Bentley and C. Wolf, *J. Org. Chem.*, 2014, **79**, 6517–6531; (d) S. L. Pilicer, P. R. Bakhshi, K. W. Bentley and C. Wolf, *J. Am. Chem. Soc.*, 2017, **139**, 1758–1761.

6 Selected examples of UV/CD sensing assays: (a) X. Huang, B. H. Rickman, B. Borhan, N. Berova and K. Nakanishi, *J. Am. Chem. Soc.*, 1998, **120**, 6185–6186; (b) J. F. Folmer-Andersen, V. M. Lynch and E. V. Anslyn, *J. Am. Chem. Soc.*, 2005, **127**, 7986–7987; (c) J. F. Folmer-Andersen, M. Kitamura and E. V. Anslyn, *J. Am. Chem. Soc.*, 2006, **128**, 5652–5653; (d) H. Kim, S. M. So, C. P. Yen, E. Vinhato, A. J. Lough, J. I. Hong, H. J. Kim and J. Chin, *Angew. Chem., Int. Ed.*, 2008, **47**, 8657–8660; (e) D. Leung and E. V. Anslyn, *J. Am. Chem. Soc.*, 2008, **130**, 12328–12333; (f) L. A. Joyce, J. W. Canary and E. V. Anslyn, *Chem.-Eur. J.*, 2012, **18**, 8064–8069; (g) F. A. Scaramuzzo, G. Licini and C. Zonta, *Chem.-Eur. J.*, 2013, **19**, 16809–16813; (h) H. M. Seifert, Y.-B. Jiang and E. V. Anslyn, *Chem. Commun.*, 2014, **50**, 15330–15332; (i) F. Biedermann and W. M. Nau, *Angew. Chem., Int. Ed.*, 2014, **53**, 5694–5699; (j) L. A. Joyce, E. C. Sherer and C. J. Welch, *Chem. Sci.*, 2014, **5**, 2855–2861; (k) K. W. Bentley, P. Zhang and C. Wolf, *Sci. Adv.*, 2016, **2**, e1501162; (l) Z. A. De los Santos and C. Wolf, *J. Am. Chem. Soc.*, 2016, **138**, 13517–13520; (m) E. Badetti, K. Wurst, G. Licini and C. Zonta, *Chem.-Eur. J.*, 2016, **22**, 6515–6518; (n) P. Zardi, K. Wurst, G. Licini and C. Zonta, *J. Am. Chem. Soc.*, 2017, **139**, 15616–15619; (o) L. Chen, S. Yu, M. Xiao, Z. Huang, K. Wen, Y. Xu, F. Zhao, X. Yu and

L. Pu, *Eur. J. Org. Chem.*, 2017, 2338–2343; (p) Y.-W. Zhao, Y. Wang and X.-M. Zhang, *ACS Appl. Mater. Interfaces*, 2017, **9**, 20991–20999; (q) C. C. Lynch, Z. A. De los Santos and C. Wolf, *Chem. Commun.*, 2019, **55**, 6297–6300; (r) F. Y. Thanzeel, K. Balaraman and C. Wolf, *Nat. Commun.*, 2018, **9**, 5323; (s) S. L. Pilicer, P. R. Bakhshi, K. W. Bentley and C. Wolf, *J. Am. Chem. Soc.*, 2019, **141**, 16382–16387.

7 Selected examples of chiroptical sensing based on covalent substrate binding: (a) F. Y. Thanzeel, K. Balaraman and C. Wolf, *Nat. Commun.*, 2018, **9**, 5323; (b) S. L. Pilicer, P. R. Bakhshi, K. W. Bentley and C. Wolf, *J. Am. Chem. Soc.*, 2019, **141**, 16382–16387.

8 Selected examples of chiroptical sensing based on covalent substrate binding: (a) X. Huang, N. Fujioka, G. Pescitelli, F. E. Koehn, R. T. Williamson, K. Nakanishi and N. Berova, *J. Am. Chem. Soc.*, 2002, **124**, 10320–10335; (b) S. Superchi, R. Bisaccia, D. Casarini, A. Laurita and C. Rosini, *J. Am. Chem. Soc.*, 2006, **128**, 6893–6902; (c) L. Dutot, K. Wright, M. Wakselman, J.-P. Mazaleyrat, M. De Zotti, C. Peggion, F. Formaggio and C. Toniolo, *J. Am. Chem. Soc.*, 2008, **130**, 5986–5992See also: (d) C. Wang, C. Zeng, X. Zhang and L. Pu, *J. Org. Chem.*, 2017, **82**, 12669–12673.

9 Also see initial post of this manuscript on ChemRxiv: <https://doi.org/10.26434/chemrxiv.12671144.v1>.

10 P. Zuman, *Chem. Rev.*, 2004, **104**, 3217–3238.

11 oPA method for AA derivatization: (a) J. D. H. Cooper, G. Ogden, J. McIntosh and D. C. Turnell, *Anal. Biochem.*, 1984, **142**, 98–102; (b) W. A. Jacobs, M. W. Leburg and E. J. Madaj, *Anal. Biochem.*, 1986, **156**, 334–340.

12 Recent applications of oPA: (a) Y. Zhang, Q. Zhang, C. T. T. Wong and X. Li, *J. Am. Chem. Soc.*, 2019, **141**, 12274–12279; (b) M. Todorovic, K. D. Schwab, J. Zeisler, C. Zhang, F. Benard and D. M. Perrin, *Angew. Chem., Int. Ed.*, 2019, **58**, 14120–14124.

13 Compound **5e** is weakly fluorescent (emission maximum at 450 nm, Φ : 8.3% in MeOH/H₂O).

14 In the classic oPA labelling reactions of α AAs with alkyl thiol reagents such as **3a** and **3b**, the corresponding isoindole product **5** can slowly react with O₂ to form oxidized by-products. In comparison, **5e** with the tolyl thiolate group is stable and does not show evident decomposition in the reaction mixture within 12 hours under an air atmosphere.

15 The plot of *g*-factor vs. ee% showed a better linear relationship than the plot of molar ellipticity vs. ee% at 10 μ M (R^2 : 0.9935 vs. 0.9913, see the ESI† for details). Measurements of Ala at 5 μ M gave acceptable sensitivity at high ee values while the sensitivity dropped considerably at 2.5 μ M.

